

# Interpretation of $Y_b(10753)$ as a tetraquark and its production mechanism

Ahmed Ali\*

*Deutsches Elektronen-Synchrotron DESY, D-22607 Hamburg, Germany*

Luciano Maiani†

*T. D. Lee Institute, Shanghai Jiao Tong University, Shanghai, 200240, China and  
Dipartimento di Fisica and INFN, Sapienza Università di Roma, Piazzale Aldo Moro 2, I-00185 Roma, Italy*

Alexander Ya. Parkhomenko‡

*Department of Theoretical Physics, P. G. Demidov Yaroslavl State University, Sovietskaya 14, 150003 Yaroslavl, Russia*

Wei Wang§

*INPAC, Shanghai Key Laboratory for Particle Physics and Cosmology,  
MOE Key Laboratory for Particle Physics, School of Physics and Astronomy,  
Shanghai Jiao Tong University, Shanghai 200240, China*

(Dated: October 15, 2019)

Recently, the Belle Collaboration has updated the analysis of the cross sections for the processes  $e^+e^- \rightarrow \Upsilon(nS)\pi^+\pi^-$ ;  $nS = 1S, 2S, 3S$  in the  $e^+e^-$  center-of-mass energy range from 10.52 to 11.02 GeV, taken at the KEKB asymmetric  $e^+e^-$ -collider. A new structure, called here  $Y_b(10753)$ , with the mass  $M(Y_b) = (10752.7 \pm 5.9_{-1.1}^{+0.7})$  MeV and the Breit-Wigner width  $\Gamma(Y_b) = (35.5_{-11.3}^{+17.6+3.9})$  MeV was observed [1]. We interpret  $Y_b(10753)$  as a compact  $J^{PC} = 1^{--}$  state with a dominant tetraquark component. The mass eigenstate  $Y_b(10753)$  in our approach is a linear combination of the diquark-antidiquark and  $b\bar{b}$  components due to the mixing via gluonic exchanges in the 't Hooft diagrams, shown recently to arise in the large- $N_c$  limit. The mixing angle  $Y_b - \Upsilon(5S)$  can be estimated from  $\Gamma_{ee}(Y_b)$ , for which only a 90% C.L. upper limit is known currently. The resonant part of the dipion invariant mass spectrum in  $Y_b(10753) \rightarrow \Upsilon(1S)\pi^+\pi^-$  and the corresponding angular distribution of  $\pi^+$  in the dipion rest frame are presented. The mixing provides a plausible mechanism for  $Y_b(10753)$  production in high energy collisions from the  $b\bar{b}$  component in its Fock space. Using this framework, we work out the Drell-Yan and prompt production cross sections for  $pp \rightarrow Y_b(10753) \rightarrow \Upsilon(nS)\pi^+\pi^-$  at the LHC.

**Introduction:** Recently, Belle has reported an updated measurement of the cross sections for  $e^+e^- \rightarrow \Upsilon(nS)\pi^+\pi^-$ ;  $nS = 1S, 2S, 3S$  in the  $e^+e^-$  center-of-mass energy range from 10.52 to 11.02 GeV, taken at the KEKB asymmetric  $e^+e^-$ -collider. They observe a new structure,  $Y_b(10753)$ , in addition to the  $\Upsilon(10860)$ - and  $\Upsilon(11020)$ -resonances, having the masses and Breit-Wigner decay widths shown in Table I [1]. The measured ranges of the product  $\Gamma_{ee} \times \mathcal{B}$  (in eV) for the three final states are also shown in Table I. The global significance of the new structure is  $5.2\sigma$ . We also recall that in high statistics energy scans for the ratios  $R_{\Upsilon\pi^+\pi^-} \equiv \sigma(e^+e^- \rightarrow (\Upsilon(1S), \Upsilon(2S), \Upsilon(3S))\pi^+\pi^-)/\sigma(e^+e^- \rightarrow \mu^+\mu^-)$  and  $R_{b\bar{b}} \equiv \sigma(e^+e^- \rightarrow b\bar{b})/\sigma(e^+e^- \rightarrow \mu^+\mu^-)$ , Belle had found no new structures in their 2016 analysis [2]. In the same analysis, a 90% C.L. upper limit of 9 eV was set on  $\Gamma_{ee}$  in search of a structure around 10.9 GeV in  $R_{b\bar{b}}$  [2].

In this Letter, we interpret  $Y_b(10753)$  as a  $J^{PC} = 1^{--}$  tetraquark candidate, whose dominant component  $Y_b^0$  consists of a colored diquark-antidiquark pair  $[bq]_{\bar{3}_c}[\bar{b}\bar{q}]_{3_c}$ , bound in the  $SU(3)$  antitriplet-triplet representation [3, 4]. However, it has a small  $b\bar{b}$  component due to the mixing via gluonic exchanges in the 't Hooft diagrams. This implies that  $\Upsilon(10860)$  and  $\Upsilon(11020)$ , which are

dominantly radial  $b\bar{b}$  excitations,  $\Upsilon(5S)$  and  $\Upsilon(6S)$ , respectively, also have a small diquark-antidiquark component  $Y_b^0$  in their Fock space. Due to the proximity of the mass eigenstates  $Y_b(10753)$  and  $\Upsilon(10860)$ , we consider that the mixing is dominantly between  $Y_b^0$  and  $\Upsilon(5S)$ . This also provides a plausible interpretation of some anomalous features measured in the decays of the  $\Upsilon(10860)$ .<sup>1</sup>

We argue that the production mechanism of  $Y_b(10753)$  is from the  $b\bar{b}$  component in  $Y_b(10753)$ , which arises from the mixing  $([bq]_{\bar{3}_c}[\bar{b}\bar{q}]_{3_c} - b\bar{b})$ . A non-vanishing mixing is induced by non-planar diagrams [9], allowing the direct production of  $Y_b(10753)$  in high energy collisions. Using this, Drell-Yan [10] and prompt production cross sections [11] for  $Y_b(10753)$  are presented for the LHC. We estimate the  $Y_b - \Upsilon(5S)$  mixing angle from  $\Gamma_{ee}(Y_b)$ , for which only a 90% C.L. upper limit is known currently.

<sup>1</sup> A tetraquark interpretation had been put forward [5, 6] for the  $Y_b(10890)$ , a resonance observed by Belle more than a decade ago [7, 8], together with  $Y_b(10860)$ , identified with  $\Upsilon(5S)$ . In subsequent data by Belle [2], two states  $Y_b(10890)$  and  $\Upsilon(10860)$  were found to have the same mass within  $2\sigma$ , essentially closing the window for an additional resonance. This seems to have changed with the announcement of  $Y_b(10753)$ .

TABLE I. Measured masses and decay widths (in MeV), and ranges of  $\Gamma_{ee} \times \mathcal{B}$  (in eV) of the  $\Upsilon(10860)$ ,  $\Upsilon(11020)$ , and the new structure  $Y_b(10753)$ . The first uncertainty is statistical and the second is systematic (Belle [1]).

State	$\Upsilon(10860)$	$\Upsilon(11020)$	$Y_b(10753)$
Mass	$10885.3 \pm 1.5^{+2.2}_{-0.9}$	$11000.0^{+4.0+1.0}_{-4.5-1.3}$	$10752.7 \pm 5.9^{+0.7}_{-1.1}$
Width	$36.6^{+4.5+0.5}_{-3.9-1.1}$	$23.8^{+8.0+0.7}_{-6.8-1.8}$	$35.5^{+17.6+3.9}_{-11.3-3.3}$
$\Upsilon(1S)\pi^+\pi^-$	0.75 – 1.43	0.38 – 0.54	0.12 – 0.47
$\Upsilon(2S)\pi^+\pi^-$	1.35 – 3.80	0.13 – 1.16	0.53 – 1.22
$\Upsilon(3S)\pi^+\pi^-$	0.43 – 1.03	0.17 – 0.49	0.21 – 0.26

In contrast to the decays of  $\Upsilon(10860)$  and  $\Upsilon(11020)$ , whose dipionic transitions ( $\Upsilon(1S)$ ,  $\Upsilon(2S)$ ,  $\Upsilon(3S)$ )  $\pi^+\pi^-$  are dominated by the resonant  $Z_b^\pm(10650)$  and  $Z_b^\pm(10610)$  states [12], the decay  $Y_b(10753) \rightarrow Z_b^\pm(10650)\pi^\mp$  is kinematically forbidden, and  $Y_b(10753) \rightarrow Z_b^\pm(10610)\pi^\mp$  has a strong phase-space suppression. Thus,  $Y_b(10753)$  decays are anticipated to reflect their dominant non-resonant component. In addition, the decays  $Y_b \rightarrow (\Upsilon(1S), \Upsilon(2S), \Upsilon(3S))\pi^+\pi^-$ , being Zweig-allowed, are anticipated to have decay widths characteristic of strong interaction. Dalitz analysis in the decay  $Y_b \rightarrow \Upsilon(1S)\pi^+\pi^-$  will show a band structure in the  $m_{\pi^+\pi^-}$  invariant mass, revealing clear evidence of two scalars,  $f_0(500)$  and  $f_0(980)$ , and the tensor  $J^{PC} = 2^{++}$  meson,  $f_2(1270)$  [13]. This feature of the dipion mass spectrum, schematically shown in Fig. 2, was already worked out for the decays  $Y_b(10890) \rightarrow (\Upsilon(1S), \Upsilon(2S), \Upsilon(3S))\pi^+\pi^-$  [5, 6], but in view of the resonant ( $Z^\pm(10610)$  and  $Z^\pm(10650)$ ) contribution, the direct tetraquark component was not easy to discern in the data. In other two decays  $Y_b \rightarrow (\Upsilon(2S), \Upsilon(3S))\pi^+\pi^-$ , only the broad  $f_0(500)$ -meson is present. With higher statistics data anticipated with the Belle-II detector, this distribution, as well as other properties of  $Y_b(10753)$ , will be well measured, allowing us to discriminate the tetraquark picture from other competing mechanisms, such as a  $D$ -wave interpretation of  $Y_b(10753)$ , with a large  $S - D$  mixing [14].

#### Tetraquark- $Q\bar{Q}$ Mixing in Large- $N_c$ Approach:

As shown in [9], a mixing between a bottomonium and hidden-beauty tetraquark is induced by non-planar diagrams. Fig. 1(a) gives the lowest order in which a tetraquark pole may arise from a pure  $b\bar{b}$  state and Fig. 1(b) represents the topological structure of the non-perturbative realization of this process to order  $1/N_c^2$ .

In brief, exchanging a gluon between the two quark loops in Fig. 1(a) produces the interaction by which a genuine tetraquark pole may form in the intermediate state. Fig. 1(b) displays the non-perturbative version of Fig. 1(a). Non-planar exchanges between the two fermion

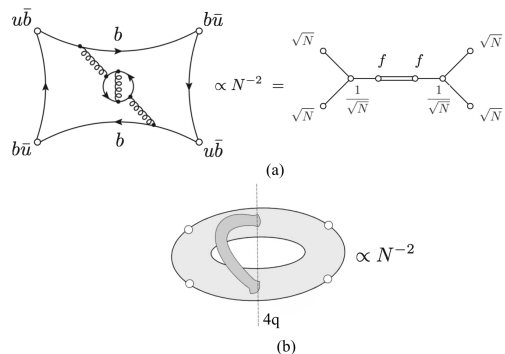


FIG. 1. (a) Left-hand side: lowest order diagram for meson-meson scattering that may have quarkonium and four-quark poles connected by mixing, as indicated by the diagram on the right-hand side, see Eq. (1). (b) Topological structure of the non-perturbative realization of the same process.  $N$  denotes the number of colors.

loops mean topologically one handle in the language introduced by 't Hooft for the large- $N_c$  expansion [15, 16] and produce a mixing coefficient  $f$  of order<sup>2</sup>

$$f = \frac{1}{N_c \sqrt{N_c}}. \quad (1)$$

**Mixing formalism:** Following [5, 6], we define the tetraquark states  $Y_b^I$  in the isospin basis, with the two isospin components  $Y_b^0 \equiv (Y_{[bu]} + Y_{[bd]})/\sqrt{2}$  and  $Y_b^1 \equiv (Y_{[bu]} - Y_{[bd]})/\sqrt{2}$  for isospin  $I = 0$  and  $I = 1$ , respectively. We ignore the mass difference due to the isospin breaking, but for the production processes isospin quantum numbers of  $e^+e^- \rightarrow Y_b^I$  are important. Since the production is via the  $b\bar{b}$ -component, which is an isosinglet, we consider only  $Y_b^0$ , the isospin-0 state. In view of the observed mass difference  $M[\Upsilon(10860)] - M[Y_b(10753)] \simeq 137$  MeV, compared to the mass difference  $M[\Upsilon(11020)] - M[Y_b(10753)] \simeq 267$  MeV, we only consider the mixing between  $\Upsilon(10860)$  and  $Y_b(10753)$ , though it can be generalized to the case of all three states.

Mass eigenstates are rotated from the eigenstates in the quark flavor space, with the latter defined as  $\Upsilon(5S)$  and  $Y_b^0$ , respectively.

$$\begin{pmatrix} Y_b(10753) \\ \Upsilon(10860) \end{pmatrix} = \begin{pmatrix} \cos \tilde{\theta} & \sin \tilde{\theta} \\ -\sin \tilde{\theta} & \cos \tilde{\theta} \end{pmatrix} \begin{pmatrix} Y_b^0 \\ \Upsilon(5S) \end{pmatrix}, \quad (2)$$

where  $\tilde{\theta}$  is a mixing angle, estimated below phenomenologically. This mixing relates  $\Gamma_{ee}[Y_b(10753)]$  and

<sup>2</sup> In the large- $N_c$  language, an amplitude  $\mathcal{A}$  for a process has the dependence  $\mathcal{A} \propto N_c^\alpha$ , where  $\alpha$  is given by  $\alpha = 2 - L - 2H$ , with  $L$  being the number of fermion loops and  $H$  the number of handles, i. e. independent non-planar sets of gluons. For a planar diagram  $H = 0$  and  $L = 1$ , yielding  $\alpha = 1$ . Large- $N_c$ -counting rules in the context of tetraquarks are given in [17].

$\Gamma_{ee}[\Upsilon(5S)]$ , yielding

$$\frac{\Gamma_{ee}[Y_b(10753)]}{\Gamma_{ee}[\Upsilon(10860)]} = \tan^2 \tilde{\theta} \kappa \left[ \frac{M[\Upsilon(10860)]}{M[Y_b(10753)]} \right]^4 \simeq 1.04 \tan^2 \tilde{\theta} \kappa, \quad (3)$$

where  $\kappa$  encodes the relative size of the (dominantly) tetraquark state  $Y_b(10753)$  and  $\Upsilon(10860)$ , the dominant  $\Upsilon(5S)$  state, which can be taken as the ratio of the square of their radial wave-functions at the origin:

$$\kappa = \left| \frac{R_{Y_b(10753)}(0)}{R_{\Upsilon(10860)}(0)} \right|^2. \quad (4)$$

Recalling that  $\Gamma_{ee}[\Upsilon(10860)] \simeq 300$  eV [13], and the present upper bound from  $R_{b\bar{b}}$ -scan on  $\Gamma_{ee}[Y_b(10753)]$  is 9 eV (at 90% C.L.) [2], lead to the upper limit

$$\tan^2 \tilde{\theta} \kappa < 0.03. \quad (5)$$

Besides the mixing coefficient (1), there should be no large factors to suppress the transition  $Y_b \leftrightarrow \Upsilon(5S)$ . In particular, we may assume the probability of finding  $b$  and  $\bar{b}$  at the same point to be smaller for the tetraquark than for  $\Upsilon(5S)$  but of the same order.<sup>3</sup> Assuming  $\kappa \simeq 1/2$ , leads to the upper limit of  $\tan \tilde{\theta} \simeq 0.25$ , yielding  $\tilde{\theta} \leq 15^\circ$ .

**Hadroproduction and Drell-Yan cross sections for  $pp \rightarrow Y_b(10753) \rightarrow \Upsilon(nS) \pi^+ \pi^-$  at the LHC:** In [11], the hadroproduction cross sections for  $\Upsilon(5S)$  and  $\Upsilon(6S)$  in  $p\bar{p}(p)$  collisions were calculated at the Tevatron and LHC, using the NRQCD framework [18] which adopts a factorization ansatz to separate the short- and long-distance effects. This was supplemented by the subsequent decays into  $\Upsilon(1S, 2S, 3S) \pi^+ \pi^-$ . We use this framework to calculate the hadroproduction cross section  $pp \rightarrow Y_b(10753) \rightarrow (\Upsilon(nS) \rightarrow \mu^+ \mu^-) \pi^+ \pi^-$  at LHC for  $\sqrt{s} = 14$  TeV.

Calculations for  $Y_b(10753)$  can be scaled from the ones for  $\Upsilon(5S)$ , as in the mixing mechanism presented here, the production takes place via the  $b\bar{b}$ -component in the  $Y_b(10753)$  Fock space, which is determined by the mixing angle, derived in the previous section. This results in the following relation:

$$\frac{\sigma_N(pp \rightarrow Y_b(10753) + X) \mathcal{B}_f(Y_b)}{\sigma_N(pp \rightarrow \Upsilon(10860) + X) \mathcal{B}_f(\Upsilon(10860))} \simeq \frac{\Gamma_{ee}(Y_b) \mathcal{B}_f(Y_b)}{\Gamma_{ee}(\Upsilon(10860)) \mathcal{B}_f(\Upsilon(10860))}, \quad (6)$$

where the r.h.s. of the above equation is measured by Belle [1], and

$$\sigma_N(pp \rightarrow \Upsilon(10860) + X) = \int dx_1 dx_2 \sum_{i,j} f_i(x_1) f_j(x_2) \times \hat{\sigma}(ij \rightarrow \langle \bar{b}b \rangle_N + X) \langle O[N] \rangle.$$

Here,  $i$  and  $j$  denote a generic parton inside a proton,  $f_a(x_1)$  and  $f_b(x_2)$  are the parton distribution functions (PDFs), for which the CTEQ6 PDFs [19] has been used in [11],  $\langle O[N] \rangle$  are the long-distance matrix elements (LDMEs),  $N$  denotes all the quantum numbers of the  $b\bar{b}$  pair, which is labelled in the form  ${}^{2S+1}L_J^c$  (color  $c$ , spin  $S$ , orbital angular momentum  $L$ , and total angular momentum  $J$ ), and  $\hat{\sigma}$  is a partonic cross section. The leading-order partonic processes for the  $S$ -wave configurations are:

$$\begin{aligned} g(p_1) g(p_2) &\rightarrow \Upsilon[{}^3S_1^1](p_3) + g(p_4), \\ g(p_1) g(p_2) &\rightarrow \Upsilon[{}^1S_0^8, {}^3S_1^8](p_3) + g(p_4), \\ g(p_1) q(p_2) &\rightarrow \Upsilon[{}^1S_0^8, {}^3S_1^8](p_3) + q(p_4), \\ g(p_1) \bar{q}(p_2) &\rightarrow \Upsilon[{}^1S_0^8, {}^3S_1^8](p_3) + g(p_4). \end{aligned} \quad (7)$$

The normalized cross sections, in which the LDMEs are factored out are defined by  $\tilde{\sigma}_N \equiv \sigma_N / \langle O[N] \rangle$ . They have been calculated in [11] for the LHC energies  $\sqrt{s} = 7, 8$  and 14 TeV. They are supplemented by the LDMEs, for which the following values have been used: The Color-Singlet LDME is  $\langle O^H {}^3S_1^1 \rangle \simeq 0.56$  GeV<sup>3</sup>, and the other two Color-Octet LDME are estimated as  $\langle O^H {}^1S_0^8 \rangle = (-0.95 \pm 0.38) \times 10^{-3}$  GeV<sup>3</sup>, and  $\langle O^H {}^3S_0^8 \rangle = (3.46 \pm 0.21) \times 10^{-2}$  GeV<sup>3</sup>. Summing over the partonic processes shown above, and using the branching ratios from the PDG, yields the cross sections  $\sigma(pp \rightarrow \Upsilon(5S) \rightarrow (\Upsilon(nS) \rightarrow \mu^+ \mu^-) \pi^+ \pi^-)$ , where  $n = 1, 2, 3$  [11].

The corresponding cross sections for the processes  $pp \rightarrow Y_b(10753) \rightarrow (\Upsilon(nS) \rightarrow \mu^+ \mu^-) \pi^+ \pi^-$  are obtained by using the scaling relation given in Eq. (6). For the LHC at  $\sqrt{s} = 14$  TeV, cross sections are given in Table II for the indicated ranges of  $p_T(Y_b)$  and rapidity  $|y|$ , separately for ATLAS and CMS and for LHCb. Theoretical uncertainties in these cross sections are almost a factor 10, dominated by the uncertainties on CO-LDMEs, as well as on the ratio on the r.h.s. in Eq. (6). To estimate the expected number of events, we use 1 pb for the cross section, which lies in the middle of the indicated ranges, yielding  $O(10^4)$  signal events at the LHCb, and an order of magnitude larger for the other two experiments, ATLAS and CMS. The discovery channel  $(\mu^+ \mu^-) \pi^+ \pi^-$ , with the  $\mu^+ \mu^-$  mass constrained by the  $\Upsilon(nS)$  ( $nS = 1S, 2S, 3S$ ) masses, involves a pair of charged pions. Thus, the background is a stumbling block, but hopefully this can be overcome, with the additional constraint of the  $Y_b(10753)$  mass.

The Drell-Yan production cross sections and differential distributions in the transverse momentum and rapidity of the  $J^{PC} = 1^{--}$  exotic hadrons  $\phi(2170)$ ,  $X(4260)$  and  $Y_b(10890)$  at the hadron colliders LHC and Tevatron have been calculated in [10]. We update these calculations for the production of  $Y_b(10753)$  at the LHC for  $\sqrt{s} = 14$  TeV, and present results for  $pp \rightarrow Y_b(10753) \rightarrow (\Upsilon(nS) \rightarrow \mu^+ \mu^-) \pi^+ \pi^-$  taking into account the current

<sup>3</sup> Unlike the case of the mixing between a molecular  $X(3872)$  and  $\chi_{c1}(2P)$  states.

mass of  $Y_b(10753)$  and the measured quantity  $\Gamma_{ee} \times \mathcal{B}$ , whose ranges are measured by Belle [1] and given in Table I. In deriving the distributions and cross sections, we have included the order  $\alpha_s$  QCD corrections, resummed the large logarithms in the small transverse momentum region in the impact-parameter formalism, and have used two sets of parton distribution functions: MSTW (Martin-Stirling-Thorne-Watt) PDFs [20] and CTEQ10 [21]; the details can be seen in [10]. Numerical results for the cross section are given in Table II, where the  $p_T$  and rapidity  $|y|$  ranges for the ATLAS and CMS, and for the LHCb, are indicated. These cross sections yield  $O(300)$  events for the current ATLAS/CMS luminosity ( $140 \text{ fb}^{-1}$ ), and  $O(10)$  events for the LHCb ( $9 \text{ fb}^{-1}$ ), but could be higher by a factor 2. The Drell-Yan cross sections are theoretically more accurate, but suffer from the small rates compared to the hadroproduction cross sections at the LHC.

**Dipion invariant mass spectra and angular distributions in  $Y_b \rightarrow \Upsilon(nS) \pi^+ \pi^-$ :** The decay amplitudes have been calculated in [6] as a sum of the Breit-Wigner resonances and non-resonating continuum contributions, with the latter adopted from [22]. The differential cross section is then written as [6]:

$$\begin{aligned} \frac{d^2 \sigma_{\Upsilon(1S)PP'}}{dm_{PP'} d\cos\theta} &= \frac{\lambda^{1/2}(s, m_\Upsilon^2, m_{PP'}^2) \lambda^{1/2}(m_{PP'}^2, m_P^2, m_{P'}^2)}{384\pi^3 s m_{PP'} [(s - m_{Y_b}^2)^2 + m_{Y_b}^2 \Gamma_{Y_b}^2]} \\ &\times \left\{ \left( 1 + \frac{(q \cdot p)^2}{2s m_\Upsilon^2} \right) |\mathcal{S}|^2 \right. \\ &+ 2 \text{Re} \left[ \mathcal{S}^* \left( \mathcal{D}' + \frac{(q \cdot p)^2}{2s m_\Upsilon^2} \mathcal{D}'' \right) \right] \left( \cos^2 \theta - \frac{1}{3} \right) \\ &+ |\mathcal{D}|^2 \sin^2 \theta \left[ \sin^2 \theta + 2 \left( \frac{q_0^2}{s} + \frac{p_0^2}{m_\Upsilon^2} \right) \cos^2 \theta \right] \\ &\left. + \left( |\mathcal{D}'|^2 + \frac{(q \cdot p)^2}{2s m_\Upsilon^2} |\mathcal{D}''|^2 \right) \left( \cos^2 \theta - \frac{1}{3} \right)^2 \right\}, \quad (8) \end{aligned}$$

where  $\lambda(x, y, z) \equiv (x - y - z)^2 - 4yz$ ,  $q_0$  and  $p_0$  are the energies of the  $Y_b$ - and  $\Upsilon(1S)$ -mesons in the  $PP'$  rest frame, respectively,  $\Gamma_{Y_b}$  is the decay width of  $Y_b$ , and  $m_{Y_b}$ ,  $m_\Upsilon$ ,  $m_P$  and  $m_{P'}$  are the masses of  $Y_b$ ,  $\Upsilon(1S)$ ,  $P$  and  $P'$ , respectively.

The  $S$ -wave amplitude for the  $PP'$  system,  $\mathcal{S}$ , and the  $D$ -wave amplitudes,  $\mathcal{D}$ ,  $\mathcal{D}'$  and  $\mathcal{D}''$ , are the sums over possible isospin states:

$$\mathcal{M} = \sum_I \mathcal{M}_I \quad \text{for } \mathcal{M} = \mathcal{S}, \mathcal{D}, \mathcal{D}', \mathcal{D}'', \quad (9)$$

where  $I = 0$  for  $\pi^+ \pi^-$ ,  $I = 0, 1$  for  $K^+ K^-$ , and  $I = 1$  for  $\eta \pi^0$ . Details are given in [6].

We concentrate on the process  $Y_b(10753) \rightarrow \Upsilon(1S) \pi^+ \pi^-$ , in which the  $\sigma = f_0(500)$ ,  $f_0(980)$ , and  $f_2(1270)$  resonances contribute. The  $I = 0$  amplitudes are given by the combinations of the resonance amplitudes,  $\mathcal{M}_0^S$  and  $\mathcal{M}_0^{f_2}$ , and the non-resonating continuum

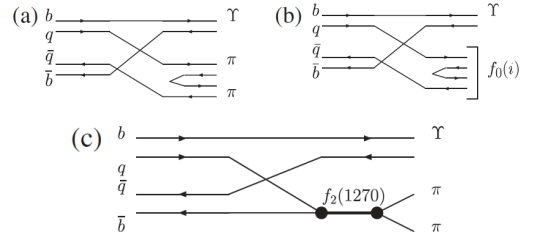


FIG. 2. Feynman diagrams for the decay  $Y_b \rightarrow \Upsilon(1S) \pi^+ \pi^-$ , where  $Y_b$  is a tetraquark state. Here,  $f_0(i)$  represents the tetraquark scalars  $\sigma = f_0(500)$  and  $f_0(980)$  [5].

amplitudes,  $\mathcal{M}_0^{1C}$  and  $\mathcal{M}_0^{2C}$ :

$$\begin{aligned} \mathcal{S}_0 &= \mathcal{M}_0^{1C} + (k_1 \cdot k_2) \sum_S \mathcal{M}_0^S, \quad \mathcal{D}_0 = |k|^2 \mathcal{M}_0^{f_2}, \\ \mathcal{D}'_0 &= \mathcal{M}_0^{2C} - \mathcal{D}_0, \quad \mathcal{D}''_0 = \mathcal{M}_0^{2C} + \frac{2q_0 p_0}{(q \cdot p)} \mathcal{D}_0, \quad (10) \end{aligned}$$

where  $S$  runs over possible  $I = 0$  scalar resonances, and  $|k|$  is the magnitude of the  $\pi^+$ -meson three momentum in the  $\pi^+ \pi^-$  rest frame. The  $m_{\pi^+ \pi^-}$  and  $\cos \theta$  distributions for  $e^+ e^- \rightarrow Y_b \rightarrow \Upsilon(1S) \pi^+ \pi^-$ , normalized by the measured cross section  $\sigma_{\Upsilon(1S) \pi^+ \pi^-}^{\text{Belle}} = (1.61 \pm 0.16) \text{ pb}$  of the older Belle data [7] were fitted in [6], which determined various coupling constants. Since these distributions are not available for the new Belle data [1], we show in Fig. 3 only the resonant contributions, using the relevant input parameters from [6]. This illustrates the anticipated spectral shapes, which will be modified in detail as the non-resonant contribution is included. The fit can only be undertaken as the experimental measurements become available.

As only the products  $\Gamma_{ee} \times \mathcal{B}$  are measured by Belle, and currently upper limits are known on  $\Gamma_{ee}[Y_b(10753)]$ , only lower bounds on the  $\mathcal{B}$ , for three dipionic final states can be derived. The corresponding lower ranges are (1.3–5.2)% for  $\mathcal{B}_{\Upsilon(1S) \pi^+ \pi^-}$ , (5.9–13.5)% for  $\mathcal{B}_{\Upsilon(2S) \pi^+ \pi^-}$ , and (2.3–2.8)% for  $\mathcal{B}_{\Upsilon(3S) \pi^+ \pi^-}$ . They are in a reasonable range for the Zweig-allowed decays, but hint that  $\Gamma_{ee}[Y_b(10753)]$  is probably close to its present 90% C.L. upper limit.

**Summary:** We have presented a tetraquark-based interpretation of the Belle data on the new structure  $Y_b(10753)$  in  $e^+ e^-$  annihilation, invoking a tetraquark- $b\bar{b}$  mixing mechanism in the large- $N_c$  limit. The  $b\bar{b}$ -component is used to predict the hadroproduction and Drell-Yan cross sections at the LHC. A crucial test of our model is in the  $m_{\pi^+ \pi^-}$  and  $\cos \theta$  distributions, whose resonant contribution is worked out, which is not expected in other dynamical schemes, such as  $Y_b(10753)$  interpreted as a  $D$ -wave  $b\bar{b}$  state, with a very large  $D-S$  mixing [14]. The tetraquark- $Q\bar{Q}$  mixing scheme suggested here has wider implications.

TABLE II. Total cross sections (in pb) for the processes  $pp \rightarrow Y_b(10753) \rightarrow (\Upsilon(nS) \rightarrow \mu^+\mu^-)\pi^+\pi^-$  ( $n = 1, 2, 3$ ) at the LHC ( $\sqrt{s} = 14$  TeV), assuming the transverse momentum range  $3 \text{ GeV} < p_T < 50 \text{ GeV}$ . The rapidity range  $|y| < 2.5$  is used for ATLAS and CMS, and the rapidity range  $2.0 < y < 4.5$  is used for the LHCb. The error estimates in the QCD production are from the variation of the central values of the CO-LDMEs and the various decay branching ratios, as discussed in Ref. [11]. Contributions from  $\Upsilon(1S, 2S, 3S)$  are added together in the Drell-Yan production mechanism as in Ref. [10].

	QCD (gg)			Drell-Yan
	$n = 1$	$n = 2$	$n = 3$	DY
LHC 14	[ 0.29, 3.85]	[ 0.70, 4.78]	[ 0.45, 3.10]	[0.002, 0.004]
LHCb 14	[ 0.08, 1.21]	[ 0.20, 1.51]	[ 0.13, 0.99]	[0.001, 0.002]

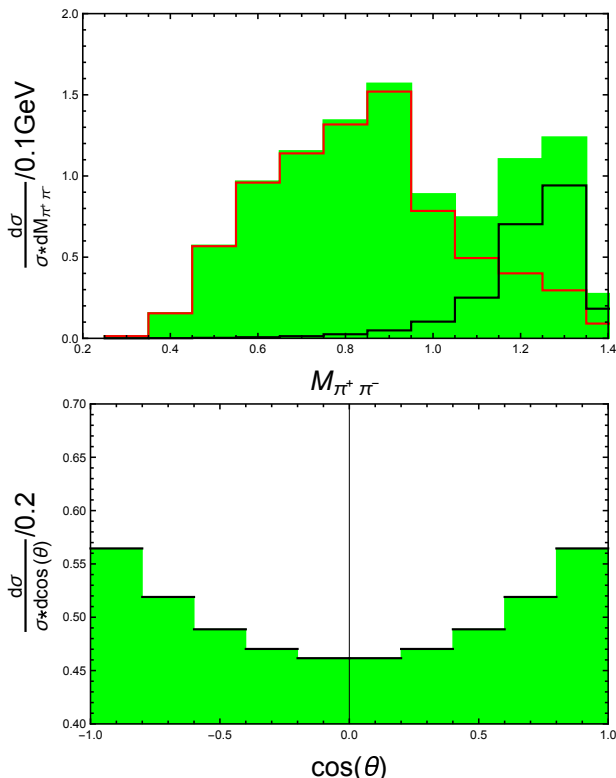


FIG. 3. The normalized resonant  $m_{\pi^+\pi^-}$  (upper plot) and  $\cos\theta$  (lower plot) distributions for  $e^+e^- \rightarrow Y_b(10753) \rightarrow \Upsilon(1S)\pi^+\pi^-$  are shown using the coupling constants obtained in [6] (green histogram). The contributions from  $f_0(500)$  and  $f_0(980)$  (left red curve) and  $f_2(1270)$  (right black curve) are indicated in the upper plot.

We thank Satoshi Mishima for his help in checking our code for the distributions shown in Fig. 3 and helpful correspondence, and the T. D. Lee Institute and INPAC, Shanghai Key Laboratory for Particle Physics and Cosmology, for supporting the Workshop on Exotic Hadrons, which stimulated the work reported here. The work of W.W. is supported in part the National Natural Science Foundation of China under Grant Nos. 11575110, 11655002, 11735010, and the Natural Science Foundation of Shanghai under Grant No. 15DZ2272100. A.P. and W.W. acknowledge financial support by the Russian Foundation for Basic Research and National Natural

Science Foundation of China according to the joint research project (Nos. 19-52-53041 and 1181101282). This research is partially supported by the ‘‘YSU Initiative Scientific Research Activity’’ (Project No. AAAA-A16-116070610023-3).

\* Email: ahmed.ali@desy.de

† Email: luciano.maiani@cern.ch

‡ Email: parkh@uniyar.ac.ru

§ Email: wei.wang@sjtu.edu.cn

- [1] R. Mizuk *et al.* [Belle Collaboration], [arXiv:1905.05521v4 [hep-ex]].
- [2] D. Santel *et al.* [Belle Collaboration], Phys. Rev. D **93**, 011101 (2016) [arXiv:1501.01137 [hep-ex]].
- [3] R. L. Jaffe and F. Wilczek, Phys. Rev. Lett. **91**, 232003 (2003) [hep-ph/0307341].
- [4] L. Maiani, F. Piccinini, A. D. Polosa and V. Riquer, Phys. Rev. D **71**, 014028 (2005) [hep-ph/0412098].
- [5] A. Ali, C. Hambrock and M. J. Aslam, Phys. Rev. Lett. **104**, 162001 (2010) Erratum: [Phys. Rev. Lett. **107**, 049903 (2011)] [arXiv:0912.5016 [hep-ph]].
- [6] A. Ali, C. Hambrock and S. Mishima, Phys. Rev. Lett. **106**, 092002 (2011) [arXiv:1011.4856 [hep-ph]].
- [7] K. F. Chen *et al.* [Belle Collaboration], Phys. Rev. Lett. **100**, 112001 (2008) [arXiv:0710.2577 [hep-ex]].
- [8] I. Adachi *et al.* [Belle Collaboration], arXiv:0808.2445 [hep-ex].
- [9] L. Maiani, A. D. Polosa and V. Riquer, Phys. Rev. D **98**, 054023 (2018) [arXiv:1803.06883 [hep-ph]].
- [10] A. Ali and W. Wang, Phys. Rev. Lett. **106**, 192001 (2011) [arXiv:1103.4587 [hep-ph]].
- [11] A. Ali, C. Hambrock and W. Wang, Phys. Rev. D **88**, 054026 (2013) [arXiv:1306.4470 [hep-ph]].
- [12] A. Bondar *et al.* [Belle Collaboration], Phys. Rev. Lett. **108**, 122001 (2012) [arXiv:1110.2251 [hep-ex]].
- [13] M. Tanabashi *et al.* [Particle Data Group], Phys. Rev. D **98**, 030001 (2018).
- [14] A. M. Badalian, B. L. G. Bakker and I. V. Danilkin, Phys. Atom. Nucl. **73**, 138 (2010) [arXiv:0903.3643 [hep-ph]].
- [15] G. 't Hooft, Nucl. Phys. B **72**, 461 (1974).
- [16] G. 't Hooft, Nucl. Phys. B **75**, 461 (1974).
- [17] A. Ali, L. Maiani, and A. D. Polosa, *Multiquark Hadrons*. Cambridge University Press, Cambridge, 2019.
- [18] G. T. Bodwin, E. Braaten and G. P. Lepage, Phys. Rev. D **51**, 1125 (1995) Erratum: [Phys. Rev. D **55**, 5853 (1997)] [hep-ph/9407339].

- [19] P. M. Nadolsky *et al.*, Phys. Rev. D **78**, 013004 (2008) [arXiv:0802.0007 [hep-ph]].
- [20] A. D. Martin, W. J. Stirling, R. S. Thorne and G. Watt, Eur. Phys. J. C **63**, 189 (2009) [arXiv:0901.0002 [hep-ph]].
- [21] H. L. Lai *et al.*, Phys. Rev. D **82**, 074024 (2010) [arXiv:1007.2241 [hep-ph]].
- [22] L. S. Brown and R. N. Cahn, Phys. Rev. Lett. **35**, 1 (1975).